Econ. Environ. Geol.
Vol. 28, No. 6, p. 623-633, 1995.

Studies on the Geology and Geochemistry in the Beonam Mine, Korea

Jae-Il Chung*, Choon-Ki Na**, Young-Up Lee*,
Seo-Ryeong Jeon* and Seon-Young Kim*

ABSTRACT: The Beonam deposits which is located in south-western part of Sobaeksan massif are emplaced along N20~30°E trending fissures in Precambrian Sobaeksan gneiss complex. Surrounding granites are inferred to be differentiated and formed from calc-alkaline magma which was generated from remelting or partial melting of the crustral material having igneous composition. The Sr isotope data of ore minerals showing significantly low initial Sr value relative to those of surrounding granite batholiths suggest that the ore-bearing fluid formed the Beonam Au-Ag mine are isotopically distinct from those of the wall rocks, and it indicates that there is no evidence of genetic relationship between ore-bearing fluids and surrounding granites, although further study should be needed. The results of paragenetic studies suggest three stages of hydrothermal mineralization; stage I: base-metal sulfides stage, stage II: late base-metal sulfides, electrum and silver-bearing sulfosalts stage, stage III: minor silver-bearing minerals, barren quartz and carbonates stage. The temperature, salinity and pressure of the Beonam deposits estimated from mineral assemblage, chemical composition, fluid inclusion and sulfur isotope geothermometry are as follows; stage I: 200~315℃, 3.5~6.5 NaCl eq. wt.%, 0.28~0.61 Kbar, stage II: 150~235℃, 4.5~7.4 NaCl eq. wt.%, 0.11~0.15 Kbar. The estimated oxygen and sulfur fugacity during first stage mineralization, based on phase relation of associated minerals, range from $10^{-35.1}$~$10^{-39.7}$ atm. and $10^{-11.0}$~$10^{-13.4}$ atm., respectively. All these evidences suggest that the Beonam deposits are polymetallic meso-epithermal ore deposits.

INTRODUCTION

A series of gold-silver ore deposits centrally located in the Namwon granite occurs in the Chinangun and Changsugun district, Chonbuk, Korea. Gold-silver ore body in these areas is mainly distributed in the vicinity of Sunchang foliated granite body, and partially occur fissure-filling quartz veins with gold-silver of the pre-Cambrian gneiss complex, locating northward the Namwon granite. In the respect of such distribution characteristics, the foliated granite body is considered as the main host of the related igneous rocks associated with gold-silver ore deposits, and some of ores have inferred to make close relation with the Namwon granite (Kim and Lee, 1984). The Beonam mine is located in Eogueri, Beonammyeon, Changsugun, Chonbuk, Korea (north latitude 127°32′27″, longitude 35°31′40″) and belongs to the Chinan-Changsu mineralization province. The mine was actively exploited to the target of 3 sets of ore veins with vertical shafts in the time of Japanese imperialism. After the Liberation of Korea, ore minerals were prospected, excavated and mined to the direction of N20°E at 350 m below sea level of Maebongjae, but stopped mining presently. According to prospecting data of KMPC (1987), the contents of Au and Ag are 5.3~19.1 g/t and 8~51 g/t respectively.

The geology and ore deposits of the study area were reported by the KMPC (1987), Lee (1989) and Yoon and Shimazaki (1993) and Chung *et al.* (1994) to the point of temperature at genesis of ore deposits, but do not have stuided the detailed origin and paragenesis of ore mineralization systematically. The geologic map including this area was not printed yet, but those such as Unbong sheet (Kim *et al.*, 1964), Osu sheet (Kim *et al.*, 1984) and Namwon sheet (Kim and Lee, 1984) in the vicinity of this area are used for references. The purpose of this study is focused the genesis and the geochemical charecteristics of Au-Ag mineralization in the Beonam mine by the settlement of geologic setting of surrounding area, by the investigation of the geochemistry, deposition and occurrence of ore minerals, and by the examination of the mineral and chemical composition, and the mineral paragenesis, the fluid inclusions and the sulfur isotopes at each ore mineralization stages.

GEOLOGY AROUND THE BEONAM MINE

The geology of the Beonam mine consists of the

* Department of Geology, Chonbuk National University, Chonju 560-756, Korea
** Department of Environmental Eng., Mokpo National University, Chonnam 534-729, Korea

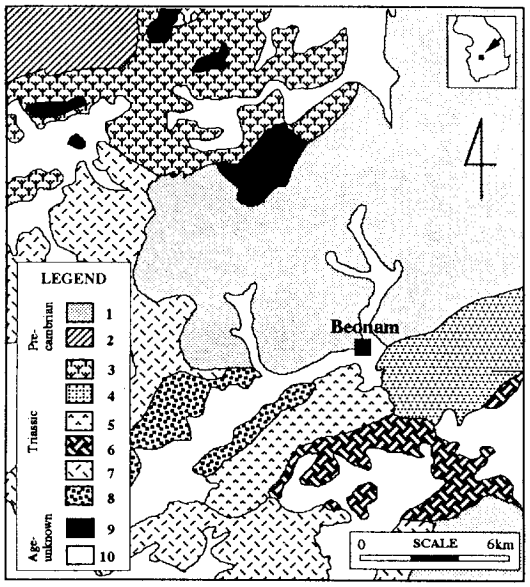

Fig. 1. Geologic map of the Beonam mine area (1; Biotite gnesis, 2; Granitic gnesis, 3; Sunchang foliated granite, 4; Leucocratic foliated granite, 5; Hornblend-biotite granite, 6; Porpyritic granite, 7; Biotite granite, 8; Two-mica granite, 9; Amphibolite, 10; Alluvium).

Precambrian Sobaeksan gneiss complex, intruded the Triassic Sunchang foliated granites, Namwon granite, the Jurassic amphibolite and the mafic and acidic dykes (Fig. 1).

Centered the mine, the Sobaeksan gneiss complex is distributed regionally and consists biotite gneiss, granitic gneiss and phophyroblastic gneiss subordinated with hornblende schist and marble. The biotite gneiss is most abundunt and is intruded by Namwon granite and age-unknown pegmatite dykes. This rock type is generally coarse-grained and foliated, but more and less disturbed. The variations of strike and dip of foliations indicate that this area was undergone the several folding movement. Under polarizing microscope, quartz grains of biotite gneiss almost show undulatory extinction and partly recrystallization which in fine grained quartz caused to develope sutured structure. Plagiclase grains of biotite gneiss occur euhedral to subhedral coarse crystal which mostly have albite twinning and partly undergo sericitization by deep alteration. And also it is bended along the boundary of fracture and eroded with micas, and discriminated from newly formed crystal which show relatively clean.

The Sunchang foliated granites is distributed as large batholith in the northwestern part of the mine, and although locally somewhat differ in rock types, consists almost of foliated medium to coarse grained rocks which partly show porpyroblastic structure. The main mineralogy of foliation consists of biotite, muscovite and hornblende, and subordinatly chlorite and epidote. Quartz and plagioclase also show cataclastic structures streched to the direction of foliations. The main strike and dip of folations are N10-40°E, 60°SE respectively. Phenocrysts consist of plagioclase, and its elliptical shapes or augen structures seems to be syntectonic origin, because it is oriented almost equal to the direction of foliations. This rock mass intrudes gneiss complex and is intruded by foliated porphyry granite and Jurassic igneous rocks.

The Namwon granite body is distributed as a batholith in the southern part of the mine, and intrudes gneiss complex and Sunchang foliated granites and is intruded by hornblende diorite. This rock mass is divided four types by its mineral texture and composition, and the time of intrusion as hornblende-biotite granite, porphyritic granite, biotite granite and two-mica granite. On the basis of its geochemical properties, it seems to be formed by magmatic differentiation as hornblende-biotite granite → porphyritic granite → biotite granite → and two-mica granite in intrusion order. The main rock type of the Namwon granite batholith is biotite granite, but hornblende-biotite granite and porphyritic granite are distributed along eastern boundary, and two-mica granite partly at northeastern part and along western boundary as a small stock showing zoned structure.

The amphibolite is small irregular pillar-like intrusive rock mass, and is distributed at Seokcheonri and Gyodongri, Changsueup, the northwestern part of the mine. This rock mass mainly consists coarse-grained hornblende, but in the same rock mass its textures greatly vary from coarse-grained to fine-grained and from massive to slightly foliated.

Dyke rocks such as basic dykes with plagioclase, hornblende and biotite, andesitic intermediate dykes, and acidic dykes with quartz, plagioclase and muscovite intrude the above-mentioned rock mass in a small scale, are irregularly distributed over whole study area as mostly oriented north-northeast direction.

GEOCHEMICAL CHARACTERISTICS OF GRANITES

Intrusion Age

The igneous rocks in the vicinity of the Beonam

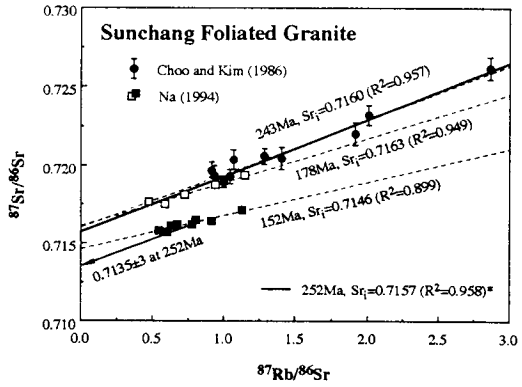

Fig. 2. Rb-Sr isochrons for the Sunchang foliated granite. Errors do not exceed site of symbols. The isochron line of 243 Ma for the Sunchung granite was reestablished with data from Choo and Kim (1986) by the omission of one sample point with significantly higher $^{87}Rb/^{86}Sr$ than the others. 252 Ma is calculated by Rb-Sr whole rock data combined those of Choo and Kim (1986) and Na (1995).

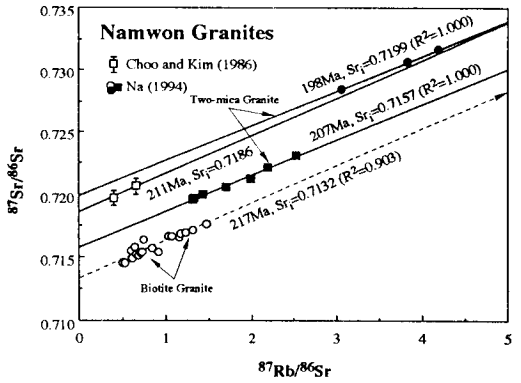

Fig. 3. Rb-Sr isochron including all whole rock analyzing data for the Namwon granite (after Na, 1995).

mine is largely divided into granites and dykes, and the nature of distribution of granites is documented and of which especially foliated granites are inferred to be related the genesis of the mine (KMPC, 1987). The granites of this area mainly consist of the Sunchang foliated granite and the Namwon granite as mentioned above (Fig. 1).

Whilst the time of intrusion of the Sunchang foliated granite measured by whole rock Rb-Sr method is 222± 5 Ma, corresponding to Triassic (Choo, 1986), that of rock forming mineral, such as biotite, muscovite and hornblende by K-Ar age dating method are range from 159 0.3 to 195 2.4 Ma (Kim, 1986). It indicates thermal alteration after the intrusion and cooling of this rocks. In addition to this, for the reexamination of the time of intrusion of this rock mass, Na (1994) applied the Rb-Sr method to both whole rock and rock forming minerals, obtained 150± 20 Ma despite of difference in initial value, and pointing out this fact, he interpreted it as alteration of whole rock as well as rock forming minerals by later metamorphism (Fig. 2). Also he reviewed the Rb-Sr isochron data of whole rock analysis which indicate the Triassic age, found out the distortion of isochron curve by one of comprising samples, reestablished the isochron curve without it and got 243 Ma. However, this reconstructed age also seems not to be geologically meaningful because of high analytical error and data dispersion (Fig. 2). Although it seems to be difficult to get the exact intrusion age of this rock mass by use of Rb-Sr or K-Ar method due to disturbance of metamorphism, but above results indicate that the Sunchang foliated granite intruded at least prior to 222 Ma, that is early Triassic or Permian time, and was reequilibriated or distorted the Rb-Sr system in the rock forming minerals and apart of whole rock by later metasomatism.

The intrusion age of the Namwon granite measured by whole rock Rb-Sr method is 211± 3 Ma (Choo and Kim, 1986), and that of hornblende by K-Ar method is 203± 10.2 Ma, relevant to early Jurassic (Kim and Lee, 1988). It indicates that the Namwon granite is early or late Triassic intrusive rock mass. Na (1994) applied the Rb-Sr method to biotite granite which comprise main rock type of Namwon granite and two-mica granite known as latest differentiation products, and as a result he showed that the former does not form isochron curve because of narrow range of $^{87}Rb/^{86}Sr$ and scatter of data, but roughly converges 217 Ma, and the latter forms isochron curve converging 207 Ma and 198 Ma in spite of broad discrepancy of initial value (Fig. 3). The inferred age of 207 Ma is consistent and well within error of those obtained from early researchers although the initial $^{87}Sr/^{86}Sr$ value is significantly discrepant, shown by high scatter of data points, that is, whilst the initial value of preexisting data is 0.7186, that of present data is inferred to be 0.7199~0.7157 for two-mica granite, and 0.7132 for biotite granite. The intrusive age of the two-mica granite, nevertheless, strongly suggests that it is close to the average value of the whole rock measurement, 207± 7 Ma. However, it should be noted that the biotite granite is the representative rock type of the Namwon granite batholith and is interpreted to be intruded earlier than the two mica facies (Hong *et al.*, 1988). Therefore, the already

Table 1. Chemical composition analysis of rocks by XRF.

	SiO_2	Al_2O_3	FeO	Fe_2O_3	MgO	CaO	Na_2O	K_2O	TiO_2	P_2O_5	MnO	Total	A/CNK
SC-1	65.84	17.04	2.18	1.53	1.75	3.58	3.25	4.14	0.47	0.12	0.06	99.96	1.043
SC-2	66.17	16.38	2.26	1.25	2.33	3.18	3.25	4.21	0.57	0.13	0.12	99.85	1.044
SC-3	62.72	17.43	2.22	2.27	2.99	4.57	3.24	2.86	0.72	0.13	0.10	99.25	1.021
SC-4	66.92	16.34	1.79	1.63	1.82	3.91	3.38	2.45	0.56	0.11	0.06	98.97	1.066
SC-5	63.19	17.58	2.60	2.42	2.57	4.36	3.39	2.25	0.56	0.17	0.16	99.25	1.103
LC-1	72.36	16.34	0.82	0.03	0.18	1.14	3.79	4.77	0.12	0.05	0.01	99.61	1.213
LC-2	64.67	18.93	1.36	0.05	0.74	3.46	4.78	4.79	0.47	0.14	0.05	99.44	0.979
LC-3	75.73	13.65	1.58	0.09	0.21	0.47	2.76	5.24	0.18	0.03	0.03	99.97	1.233
LC-4	71.17	15.34	1.31	0.06	0.42	1.45	3.43	5.56	0.29	0.07	0.03	100.13	1.073
LC-5	71.01	15.21	1.62	0.11	0.63	2.23	3.90	4.12	0.29	0.08	0.04	99.24	1.019
MG-1	74.32	14.54	0.47	0.12	0.32	0.71	3.39	4.72	0.12	0.21	0.03	98.95	1.214
MG-2	74.36	14.85	0.44	0.08	0.23	0.72	3.49	4.82	0.11	0.14	0.02	99.26	1.210
MG-3	72.52	15.32	1.02	0.27	0.24	0.81	3.54	5.49	0.10	0.11	0.04	99.46	1.157
MG-4	75.27	14.32	1.31	0.04	0.16	0.39	3.76	3.64	0.06	0.21	0.05	99.21	1.322
MG-5	76.92	15.73	0.72	0.04	0.15	0.58	2.15	3.33	0.07	0.06	0.02	99.77	1.919
HB-1	68.62	15.78	2.47	0.65	1.06	2.66	3.07	4.92	0.32	0.08	0.05	99.68	1.037
HB-2	64.88	16.30	3.84	0.93	2.05	3.38	3.72	3.64	0.64	0.13	0.07	99.58	1.006
HB-3	69.13	15.14	2.57	0.89	1.42	2.67	3.32	2.94	0.45	0.12	0.04	98.69	1.121
HB-4	67.07	15.89	3.07	0.82	1.55	2.91	3.21	4.54	0.51	0.12	0.07	99.76	1.026
HB-5	68.78	15.34	2.45	0.64	1.18	2.92	3.43	2.96	0.42	0.11	0.06	98.29	1.083
PP-1	68.72	15.17	3.62	0.64	0.64	3.46	3.45	2.05	0.54	0.14	0.07	98.50	1.069
PP-2	69.73	15.92	2.48	0.83	1.51	2.49	3.57	3.75	0.31	0.08	0.05	100.72	1.101
PP-3	68.52	15.64	2.92	0.96	1.01	3.22	3.87	2.88	0.44	0.11	0.09	99.96	1.020
PP-4	68.20	15.75	3.04	0.82	1.02	2.97	3.71	3.53	0.37	0.11	0.07	99.59	1.028
PP-5	68.63	15.44	3.54	0.53	0.90	2.61	3.36	3.98	0.72	0.10	0.08	99.89	1.059
Bt-1	72.57	14.77	1.82	0.23	0.57	2.39	3.74	3.29	0.31	0.07	0.05	99.81	1.051
Bt-2	72.84	14.75	1.38	0.16	0.52	2.01	3.39	3.45	0.24	0.71	0.03	99.48	1.138
Bt-3	73.44	14.71	1.37	0.22	0.41	1.89	3.97	3.56	0.21	0.08	0.02	99.88	1.064
Bt-4	73.16	14.67	1.69	0.08	0.38	1.91	3.93	3.67	0.24	0.09	0.02	99.84	1.055
Bt-5	71.87	14.79	2.08	0.35	0.61	2.52	3.24	3.54	0.20	0.08	0.03	99.31	1.076
TM-1	74.98	14.32	1.37	0.05	0.29	1.32	3.97	2.38	0.14	0.06	0.03	98.91	1.244
TM-2	73.14	15.01	1.27	0.34	0.28	1.64	3.99	3.93	0.18	0.06	0.02	99.86	1.088
TM-3	73.52	14.97	1.51	0.05	0.28	1.76	4.30	3.15	0.19	0.04	0.03	99.80	1.094
TM-4	75.64	14.01	1.33	0.02	0.19	0.84	3.63	3.37	0.12	0.05	0.04	99.24	1.257
TM-5	73.82	14.33	1.38	0.26	0.34	1.67	3.82	2.85	0.18	0.07	0.02	99.74	1.062

Abbreviations: SC; Sunchang foliated granite, LC; Leucocratic foliated granite, MG; Mangang foliated granite, HB; Hornblende-biotite granite, PP; Porphyritic granite, Bt; Biotite gnesis, TM; Two-mica granite.

documented data, 211 Ma must be regarded as an lowest limit of intrusion age, and each rock type comprising this rock mass is also regarded as a production of step-by-step intrusion with appropriate interval rather than that of successive differntiation or intrusion. It needs further study for the hornblende-biotite granite and porphyritic granite, whether those above mentioned are any significance as an intrusion age for Namwon granite batholith contentious or not.

Geochemical Properties

To examine the geochemical properties of granites, bulk rock analysis for major elements of representative samples of each rock types is carried out. Major elements are analyzed on pressed powder pellets by XRF at the University of Tsukuba, and the results of each rock types are summarized in Table 1. To show and compare the geochemical properties of major elements of each rock types, the analysis data are plotted in Harker diagram shown by Fig. 4.

In case of foliated granites, contents of SiO_2 show incresing trend from Sunchang foliated granite, leu-

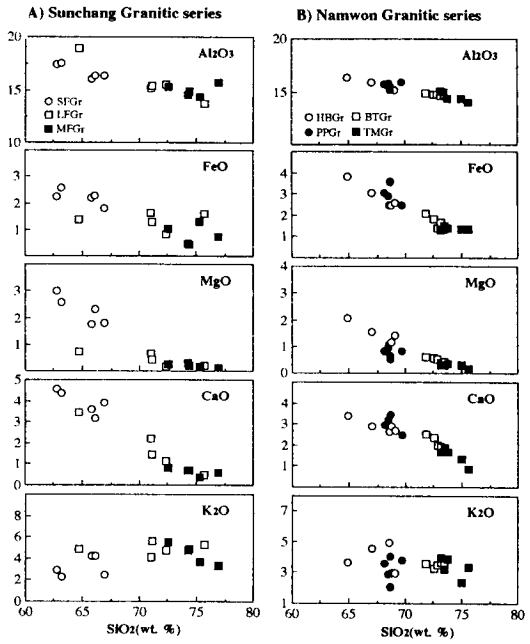

Fig. 4. A) Harker variation diagrams for the analysed samples of foliated granite. Full circle; Sunchang foliated granite, open circle; leucocratic foliated granite, open square; Mangang foliated granite. B) Harker variation diagrams for the analysed samples of Namwon granite. Full circle; hornblende-biotite granite, open circle; porphyritic granite, open square; biotite granite, full square; two mica granite.

cocratic foliated granite to Mangang foliated granite, so magmatic differentiation of Mangang granite seems to be more advanced than Sunchang granite. In Namwon granites the order of magmatic differentiation is advanced from hornblende-biotite granite, porphyritic granite, biotite granite to two-mica granite. Particularly in case of Namwon granites, variation of silica versus oxides of major elements is so consistent that it is suggestive to be a series of production of magmatic differentiation. This distribution characteristics of major elements correspond with the results of Hong *et al.* (1988). Based on this distribution characteristics of major elements, Hong *et al.* (1988) interpreted that four rock types comprising Namwon granites are resulted from magmatic differentiation to be ordered hornblende-biotite granite, porphyritic granite, biotite granite and two-mica granite. The geochemical distribution characteristics of major elements is general trend of it that as Al_2O_3, TiO_2, FeO, CaO and MgO contents decrease, and K_2O contents increase with increasing SiO_2, Na_2O contents display no consistent covariation with SiO_2 contents. Variation of silica vs. oxides of major elements shows that the investigated granites display a trend similar to that of the fractional crystallization of magma (Bowen, 1958), and also suggestive that this granites are products of magmatic differentiation of Calc-alkaline series.

The molar ratio of A/CNK(Al_2O_3/(Na_2O+K_2O+CaO)) of Sunchang foliated granite ranges 1.021~1.103; leucocratic foliated granite, 0.979~1.233; Mangang foliated granite, 1.157~1.919; hornblende-biotite granite, 1.006~1.121 ; porphyritic granite, 1.020~1.101; biotite granite, 1.051~1.138; and two-mica granite, 1.062~1.257, and is mostly included as peraluminous (A/CNK>1), partly as metaluminous (A/CNK<1). Such a granite with peraluminous properties is known to be formed by upper earth material, especially partial melting of pelitic sediments (Lefort, 1981). And Turpin *et al.* (1990) insisted that the partial melting of meta-igneous rocks also results the peraluminous magma.

The molar ratios of A/CNK of each rock types are generally below value point 1.1, so these granites are classified petrogenetically into I-type on the basis of I/S type classification criteria (Chappell and White, 1974). But as a part of granites, especially in highly evolved granite such as leucocratic foliated granite, Mangang foliated granite and two-mica granite, show the coexisting characteristics of I-type and S-type, it is the applicative limitation of I/S type classification criteria on the granites of high SiO_2 contents as already pointed out.

In the classification of granitic magma, it is noted that the preexisting data of the investigated granite have high value of initial $^{87}Sr/^{86}Sr$ ratio, although their intrusion ages are still equivocal. According to Choo and Kim (1986) and Na (1994), the initial values of Sr in Namwon granite and foliated granite are entirely above 0.710, so those granites are included to S-type and generally considered to be generated by crustal materials. To summarize these characteristics, while the results of geochemistry of whole rock in most of granites show a trend of I-type, although a part of it have S-type, those of Sr isotope analysis a trend of strong S-type, so it indicates that this granites contain two fold properties of I/S type. These characteristics together with peraluminous properties of the elemental geochemistry mentioned above strongly suggest that the granites originated from differentiation products of remelting or partial melting magma of meta-igneous rocks.

It is clear that the granites occurred in the vicinity of the Beonam mine do not fit neatly into either the

I/S series criteria. Being considered only the geochemistry of major elements, these granites are classified into I-type granite (Table 1), but in the light of Sr isotope, these granites are classified typically into S-type granite series. It is assumed from the intergration of isotopic and elemental data that the granites in the study area were formed by remelting or partial melting of the crustal material having an igneous composition.

ORE DEPOSIT

The gold-silver ores of the Beonam mine occur in the several sets of fissure-filling hydrothermal veins intruded the biotite gneiss. In the Beonam mine, main adit was directed with N20°E and digged out about 180 m, and in this, a single ore vein with N20°~25°E strike and 50~80°SE dip, which had the biotite gneiss as wall rocks, was deposited. The width of the ore vein is about 0.1~3 m including the fault clays. In the south-east of the main adit, three sets of ore veins were developed and had actively exploited in the time of Japanese imperialism, but investigation of these was restricted considerably, because of the submersion and the possibility of rock falls. Based on the investigation data of the adits, the ore veins are divided into those including considerable amount of pyrite and the other ones including sphalerite, pyrite, galena and chalcopyrite. The host rocks were remarkably altered by silicification and carbonatization, and weakly by rhodochrocitization, chloritization and sericitization. It is also observed that zoned structures were developed to the center of veins with variable size of euhedral pyrite and arsenopyrite → a single growth of crystal quartz (comb structures) → carbonates and microquartz → pyrite and minor amount of silver-bearing mineral. The ores associated with small amount of breccia fault occurs, and the crystal quartz was grown radially using the cavity of the host rocks as nucleus, above which were developed with vein quartz showing zoned structures which was covered with ore minerals such as carbonates, pyrite, sphalerite, chalcopyrite and galena.

ORE MINERALS

Ore minerals occurring in the Beonam Mine are pyrite, chalcopyrite, arsenopyrite, pyrrhotite, galena, sphalerite, marcasite, stannite, Au-Ag bearing minerals and magnetite etc., and gangue minerals are quartz, calcite, clay minerals, sericite, chlorite and epidote etc. Au-Ag bearing minerals are Ag-Sb sulfates, such as electrum, argentite, polybasite, pyragyrite, stepanite etc. In field and microscopic studies, the ore mineralization stage in the Beonam mine is classified into three main stages, and the deposition of main ore minerals is known to have been occurred during the mineralization stage I and II.

The stage I is a mineralization stage of dark grey quartz and most of sulfide minerals. Veins consists of large quantities of pyrites and minor sufide minerals including arsenopyrite, chalcopyrite and sphalerite, and are associated with a little of euhedral magnetite and disseminated quartz grain. Arsenopyrites are present both euhedral and subhedral in the gangue minerals. Some of it occur within the pyrite and rarely in the form of inclusion of gold-silver bearing minerals also both as euhedral and subhedral crystal. This suggests that arsenopyrites were deposited during early stage of mineralization. Pyrites are closely accompanied with the sphalerite and chalcopyrite, and occurs in the form of inclusion or as host mineral, inferring the nearly contemperaneous mineralization. In the most of sphalerites, the chalcopyrite inclusions are included, and this informs that the mineralization of it was nearly contemperaneous and continued subsequently. Pyrite mineralized in the stage I mostly shows densely fractured, and this suggests that extensive fracturing occurred after precipitation of the mineralization stage I minerals.

The stage II is a crystallizing stage of white massive quartz and minor amount of sulfides, and Au-Ag bearing minerals such as electrum, agentite, Ag-Sb sulfates. Au-Ag bearing minerals occur as inclusions within arsenopyrites and disseminated state within galena. Rarely it infills the fissurred microfracture of arsenopyrites or pyrites and occurs in the partial replacement of chalcopyrites. Au contents of electrum range 47~58 atomic% and the ratio of Au:Ag contents is typically about 1 : 1.

The stage III is a crystallizing stage of fine grained white quartz with minor pyrite and calcite, while occurs in the form of veinlets cutting off the brecciated pyrite and quartz grain or infilling the grain boundary and the fissurred fracture.

The summary of paragenesis of minerals based on the minerals and mineralization order according to the each mineralization stages is shown by Fig. 5.

Sr ISOTOPE COMPOSITION OF ORE MINERALS AND RELATING IGNEOUS ROCKS

Sr isotopic method is widely used to examine the

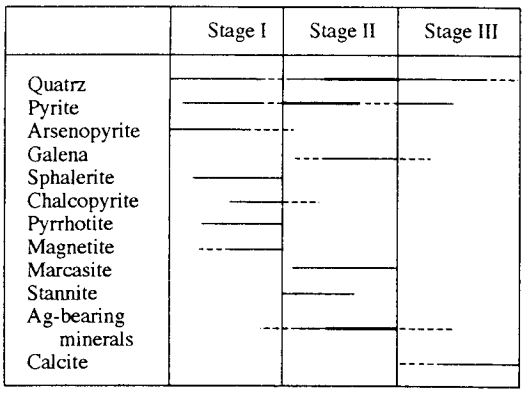

Fig. 5. Paragenetic sequence of minerals from the Beonam mine. Width of lines corresponds to relative abundance.

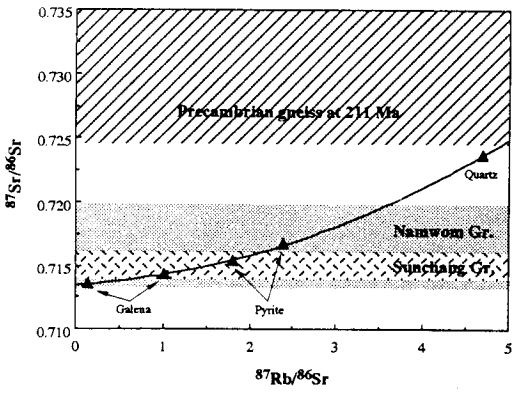

Fig. 6. $^{87}Rb/^{86}Sr$ versus $^{87}Sr/^{86}Sr$ correlation diagram for ore minerals seperated from the ore body of the Beonam mine. As can be observed, no isochron can be drawn from the experimental data. Also plotted are three domains of Sr initial ratios obtained from wall rock, precambrian gneiss and surrounding igneous rocks such as Sunchang and Namwon granite of the Beonam mine (Choo and Kim, 1986; Na, 1995).

origin of rock by its initial value as well as to determine the absolute age dating. If a rock mass is originated from syngenetic magma and evolved in closed system after intrusion and solidification, then an isochron curve is made and should be converged into the same initial value unrelated to the ratio of Rb/Sr (Faure, 1986). This fundamental idea is applied to the determination of ore deposition age as well as to the trace of relating igneous rocks subordinating the ore deposits (Brannon *et al.*, 1992; Lange *et al.*, 1983; Nakai, 1992). As above mentioned the genetically related igneous rocks with the Beonam mine is inferred to be Sunchang foliated granite only based on the features of spatial distribution, but the quantative data for this is not yet reported. Therefore, in order to acquire the quantative data whether the surrounding granite is related with the genesis of the Beonam mine and to evaluate the applicability of Sr isotopic method, the Sr isotopic ratio of ore minerals occurred in the Beonam mine is measured and compared with those of surrounding granites, and the results are reviewed. The pyrite and galena as ore minerals, and quartz as gangue mineral which occur most commonly in the Beonam mine are selected for measuring. Each mineral fractions are seperated by hand picking. The seperated minerals are powdered by agate mortar, dissolved by multi acid ($HF+HNO_3+HClO_4$), isolated Sr from other concomitant elements by conventional cation-exchange chromatography, and then analyzed the ratio of $^{87}Sr/^{86}Sr$ by solid mass spectrometer (Finnigan MAT 262) installed at the institute of geosciences, University of Tsukuba. Rb and Sr of each minerals are primarily quantified by ICP, and based on this results requantified by isotope dilution method (Geyh and Schleicher, 1990). The Sr isotopic ratios and concentrations of Rb and Sr are shown in Table 2, and the results comparison with proposed Sr initial value data of the Sunchang foliated granites and the Namwon granites are showen in Fig. 6.

Of the Sr isotopic ratio of ore minerals occurring in the Beonam mine, while those of galena range 0.713520~0.714304, and in case of quartz, those of dark grey quartz inferred to mineralize at the stage I gets 0.713881, and fine grained white quartz infer-

Table 2. Rb-Sr analytical results for various minerals in Beonam mine and calculated initial $^{87}Sr/^{86}Sr$ at 211 Ma and 252 Ma.

Sample	$^{87}Sr/^{86}Sr \pm 2\sigma(m)$	Rb	Sr	$^{87}Rb/^{86}Sr$	Init. $Sr_{(211\ Ma)}$	Init. $Sr_{(252\ Ma)}$
Quartz 1	0.713881± 10	3.92	380.6	0.0243	0.713808	0.713794
Quartz 2	0.723627± 10	2.97	1.83	4.6997	0.709524	0.706779
Galena 1	0.713520± 21	0.04	0.84	0.1485	0.713075	0.712988
Galena 2	0.714304± 14	0.35	0.99	1.0227	0.711236	0.710638
Pyrite 1	0.715382± 20	0.14	0.22	1.8096	0.709952	0.708895
Pyrite 2	0.716715± 16	0.17	0.21	2.3873	0.709552	0.708158

red to mineralize at later mineralization stage has typically the highest value, 0.723627. If these minerals were settled from the cogenetic ore-bearing fluid and the ore-bearing fluid was sustained in closed system which did not exchange the materials with surrounding wall rocks during the mineralization period and the mineralization ages of each minerals are not too different the $^{87}Sr/^{86}Sr$ and $^{87}Rb/^{86}Sr$ regressed into a single isochron showing straight line. But shown by Fig. 6, the Sr-Rb system of the ore minerals occurring the Beonam mine does not fit in an isochron, and as the mineralization stage comes later, the values of ^{87}Sr have an incresing trend comparing with equilibrium proceeding ratio. It can be inferred that the ore bearing fluid was not sustained in closed system and the Sr-Rb system of the ore-bearing fluid was disturbed by the mixing of elements extracted from surrounding wall rocks during the mineralization stage. Therefore, the Sr-Rb system of ore minerals occurring in the Beonam mine is not appropriate as a tracing tool for the dating of mineralization age. Using the intrusion age of surrounding granites inferred by the features of spatial distribution of the relating igneous rocks, however, the initial $^{87}Sr/^{86}Sr$ values of ore minerals are calculated and compared these values with those of relating igneous rock, it is possible to be evaluated the genetic relationship between ore minerals and surrounding igneous rocks. That is, if the mineralization of ore minerals occurring in this mine was mineralized from the cogenetic ore-bearing fluid with the magma which formed the relating igneous rocks, the initial $^{87}Sr/^{86}Sr$ values of two are conformable. And also if as the mineralization stage came later shown by Fig. 6, the ^{87}Sr was supplied from surrounding wall rocks having high $^{87}Sr/^{86}Sr$ value, though it was formed from the cogenetic magma, the initial Sr values of ore minerals are higher than those of relating igneous wall rocks. From this point, for the sake of the Sunchang foliated granites and the Namwon granites distributed in the vicinity of the Beonam mine is to be the relating igneous rocks, the initial Sr values of it should be the same as or lower than those of ore minerals at the same intrusion age. Nevertheless, each initial Sr values of ore minerals estimated by intrusion age of each relating igneous rocks show significantly lower than those of both granites, thus it is difficult to correlate the origin of ore minerals with these granites. Therefore, these results suggest that the ore-bearing fluids accumulating this ore deposits were originated by the concurrent granite having the initial Sr values lower than those of surrounding igneous rock mass

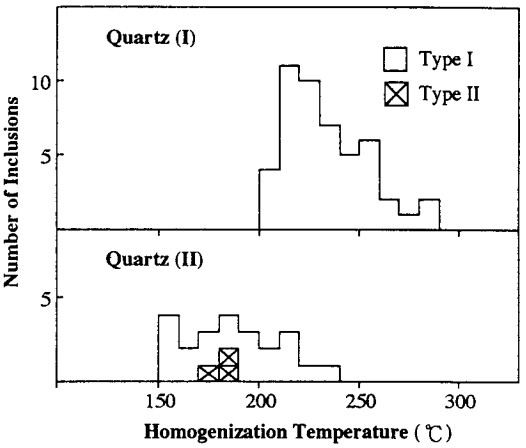

Fig. 7. Homogenization temperature of fluid inclusions in stage I, II quartz of the Beonam mine.

inferred from the features of spatial distribution.

GENESIS OF ORE DEPOSITS

The Beonam mine is the fissure-filling ore deposits occurring the several sets of hydrothermal veins located in the biotite gneiss. The main strike and dip of ore veins are N20°~30°E and 50°~80°SE. The fracture system which controlled the developement of ore veins is the same series of foliation striking N10°~40°E which is developed in host rocks such as biotite gneiss and foliated granites, and suggests that mineralization is closely related with preexisting fracture structures. Dyke rocks distributed around the mine is generally intruded along the same series of tectonic lineaments.

For the study of the temperatures of the Beonam ore minerals, the homogenization temperatures of fluid inclusions (Lee, 1989) and the sulfur isotopic geothermometer (Yoon and Shimazaki, 1993) were measured, but while the temperatures of ores estimated by the homogenization temperatures of fluid inclusions range 144~207℃, those by the sulfur isotopic geothermometer 361~677℃, so the two data are too different to compare with. In this study, however, as the homogenization temperatures of fluid inclusions included in quartz of the mineralization stage I range 200~290℃ (Fig. 7), this corresponds relatively well as correlated with 259℃, the temperatures of ore genesis based on sulfur isotopic geothermometer measured by sphalerite-pyrite couple, the paragenetic minerals of the stage I (Fig. 8). And also using the sphalerite-pyrite-arsenopyrite paragenetic mineral as-

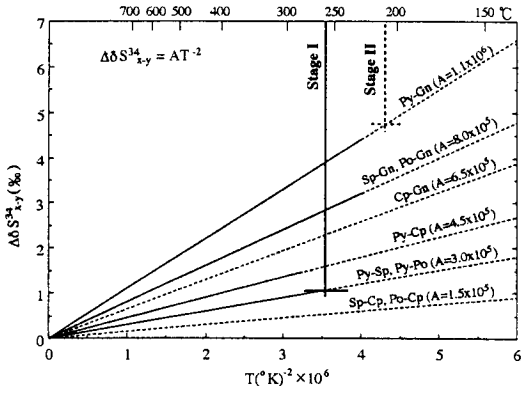

Fig. 8. Sulfur isotopic fractionation between sulfide mineral pairs depends on the temperature. Also shown the sulfur isotopic data of each mineralization stage in the Beonam deposits.

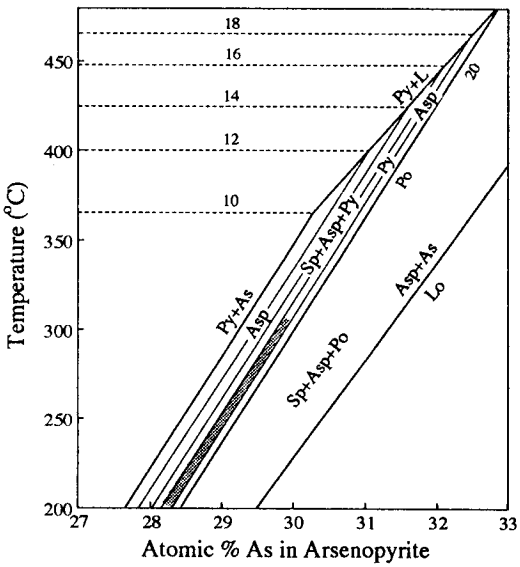

Fig. 9. Diagrom of temperature vs. As contents in arsenopyrites coexisting with pyrite and sphalerite at stage I from the Beonam mine. Contours are mole% FeS in sphalerite. Abbreviations: Asp; arsenopyrite, Lo; lollingite, Po; pyrrhotite, Py; pyrite, Sp; sphalerite, As; arsenic, L; liquid.

semblage which concurrently mineralized at the stage I and depicting the As atomic% of arsenopyrite and FeS mole% in the sphalerite in the figure suggested by Scott (1973) and Hutchison and Scott (1981), the temperatures of ore genesis is estimated, correlated with and reviewed. The temperatures estimated by equilibrium phase relationship of the paragenetic mineral assemblage are 205~315℃ which correspond

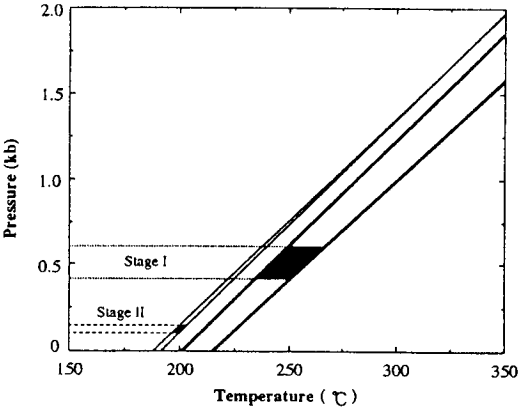

Fig. 10. The calculated isochores of stage I and II fluid inclusions at the Beonam mine and the P-T conditions for each minerizing stage of the Beonam mine determined by combining calculated isochones and sulfur isotope geothermometric data.

with the homogenization temperatures of fluid inclusions, but a high limit of temperature is a little high (Fig. 9). The homogenization temperatures of fluid inclusions in quartz which is one of representative minerals of the stage II are 150~235℃, this relatively corresponds within the range of the homogenization temperatures of fluid inclusions suggested by Lee (1989). Also the temperature measured by sulfur isotope geothermometer in galena and later pyrite couple, the paragenetic minerals representing the mineralization stage II is 213℃, and agree well with those of the homogenization temperatures of fluid inclusions. From the results mentioned above, the temperatures of ore minerals in the Beonam mine are generally estimated 200~315℃ at the mineralization stage I and 150~235℃ at the stage II, respectively.

The pressure condition of ore fluid during the ore deposition is possibly estimated by and Fe contents of sphalerite coexisted with pyrite and hexagonal pyrrhotite (Scott and Barnes, 1971; Lusk and Ford, 1978; Hutchison and Scott, 1981). In this study the pressure of ore bearing fluid estimated by calculating the equation suggested by Lusk and Ford (1978) and Hutchison and Scott (1981) substituting the Fe contents of sphalerite which is measured from the appropriate samples conincident with above condition is 0.28~0.50 Kb (Fig. 10). And also the pressure condition of ore bearing fluid is possibly estimated by the temperatures of mineral genesis and the salinity of ore fluids (Hass, 1971; Potter and Brown, 1977; Nicholls and Crowford, 1985). The pressure of ore bearing fluid estimated by P-T isochores calculated by

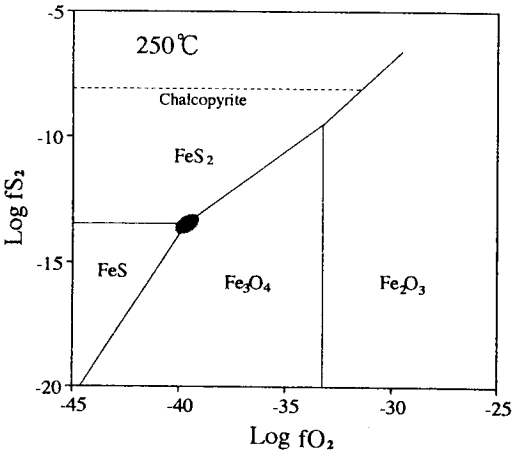

Fig. 11. Fugacity of sulfur vs. fugacity of oxygen at 250℃ showing regions stability of pyrite % pyrrohotite magnetite assemblage from the stage I of the Beonam mine.

the data input in the computer program of Nicolls and Crowford (1985) is 0.44~0.50 Kb showing the ralatively higher range than that of sphalerite geobarometer. The P-T isochores measured by the fluid inclusion data representing the stage II show the range of 0.11~0.15 Kb, and this is inferred that the pressure of the ore fluids at the stage II is much lowered that of the ore fluids at the stage I (Fig. 7).

The values of inferred partial pressure of oxygen and sufur estimated by phase diagram of the Fe-S-O system, which is based on relationship of pyrite-pyrrhotite-magnetite paragenesis and temperatures of ore genesis were yield both $10^{-39.7}$ atm. and $10^{-13.4}$ atm. at 250℃, and 10^{-35} and 10^{-11} at 300℃, respectively (Fig. 11). Considering the precipitation sequence of ore minerals, it is inferred that during the mineralization, both the falling of tempertures of mineralizing fluids and progressive decline of partial pressure of sufur and oxygen occurred.

Overall it summarizes that the Au-Ag ore mineralization in the Beonam mine is suggested to be formed from the mineralization condition of meso-epithermal type.

CONCLUSIONS

The study on the local geology and mineralization in the Beonam Au-Ag mine is summarized as following features.

1. The Beonam ore deposits are fissure filling ore deposits which infill the fracture striking N10°~40°E and consist of several sets of horizontal veins.

2. The mineralization is accomplished through three stage, and the Au-Ag bearing ore minerals accumulated at the stage II. The main Au-Ag bearing ore minerals are electrum, argentite and Ag-Sb sulfate.

3. The temperature of ore genesis and the pressure of ore fluids estimated by fluid inclusion, sulfur stable isotope, phase equilibrium relationship of paragenetic mineral assemblage range 200~315℃ and 0.28~0.61 Kb at the stage I, and 150~235℃ and 0.11~0.15 Kb at the stage II.

4. According to the above condition of ore genesis, the Beonam mine is inferred to be the ore deposits of "meso-epithermal type".

5. Surrounding granites are inferred to be differntiated and formed from calc-alkaline magma which was generated from remelting or partial melting of the crustal material having igneous composition.

6. The Sr isotope data of ore minerals showing significantly low initial Sr value relative to those of surrounding granite batholiths suggest that the ore-bearing fluids formed the Beonam Au-Ag mine are isotopically distinct from those of the wall rocks, and it indicates that there is no evidence of genetic relationship between ore-bearing fluid and surrounding granites, although further study should be needed.

ACKNOWLEDGMENTS

This research was financially supported by a grant from the Center for Mineral Resources Research.

REFERENCES

Bowen, N. L. (1958) The evolution of the igneous rocks. Princeton univ. press, Princeton.

Brannon, J. C., Podosek, F. A. and MoLimans, R. K. (1992) Alleghanian age of the Upper Mississippi Valley Zinc-Lead Deposit Determined by Rb-Sr Dating of Sphaierite. Nature, v. 356 p. 509-511.

Chappell, B. W. and White, A. J. R. (1974) Two contrasting granite types. Pecific Geology, v. 8, p. 173-174.

Choo, S. H. (1986) Rb-Sr age determination on Ryeongnam massif (III), Korea Institute of Energy and Resources, KR-86-2-17, p. 1-28.

Choo, S. H. and Kim, S. J. (1986) Rb-Sr age determination on Ryeongnam massif (II); Granitic gneiss and gneissose granites in the south-western Jirisan region. KIGAM Report, v. 7, p. 7-33 (in Korean).

Chung, J. I., Lee, Y. U., Na, C. K., Lee, K. S., Jeon, S. R. (1994) Gold-Silver Mineralization in the Beonam Mine, Chonlabukdo, Korea. Jour. Korean Earth Science Soc., v. 15, No. 6, p. 459-469.

Faure, G. (1986) Principles of isotope geology. 2nded., John Wiley & sons, Inc.

Geyh, M. A. and Schleicher, H. (1990) Absolute age de-

termination: physical and chemical dating methods and their application. Heidelberg, Springer-Verlag, p. 83.
Hass, J. L. (1971) The effect of salinity on the maximum thermal gradient of a hydrothermal system at hydrostatic pressure, Econ. Geol., v. 66, p. 940-946.
Hong, S. S., Kim, Y. J. and Kim, J. B. (1988) Petrochemical study on Namweon granite body in the Namweon area. Jour. Geol. Soc. Korea, v. 24, Special Issue, p. 132-146 (in Korean).
Hutchison, M. N. and Scott, S. D. (1981) Sphalerite geobarometry in the Cu-Fe-Zn-S system, Econ. Geol., v. 76, p. 143-153.
Kim, D. H. and Lee, B. J. (1984) Geological Map of Korea Namweon Sheet (1/50000), Korea Institute of Energy and Resources.
Kim, K. B., Choi, W. C., Hwang, J. H. and Kim, J. H. (1984) Geological Map of Korea Osu Sheet (1/50000), Korea Institute of Energy and Resources.
Kim, O. J., Hong, M. S., Yun, S. K., Park, H. I., Park, Y. D., Kim, K. T., Lee, H. Y. and Yoon, S. (1964) Geological Map of Korea Un Bong Sheet (1/50000), Geological Survey of Korea.
Kim, Y. J. (1986) Geochronology and petrogenesis on the older granitic rocks collected across the Ryeongnam massif, Korea. Jour. Korean Inst. Mining Geol., v. 19, Special Issue, p. 151-162 (in Korean).
Kim, Y. J. and Lee, C. S. (1988) The study on Igneous Rocks and their Igneous Activity in the Jangsoo-Unbong Area. The Journal of the Geological Society of Korea, v. 24, Special Issue, p. 111-131.
KMPC (1987) Report On Core Drilling, Korea Mining Promotion Corporation. No. 10, p. 184-185.
Lange, S., Chaudhuri, S. and Clauer, N. (1983) Strontium isotopic evidence for the origin of barites and sulfides from the Mississippi Valley-type ore deposits in southeast Missouri. Econ. Geol., v. 78, p. 1255-1261.
Lee, C. S. (1989) Geochemistry of granitoids and genesis of the gold-silver deposits in the Jinan-Jangsu area, Ph. D. thesis, Chonnam Nat. Univ.
Lefort, P. (1981) Manaslu leucogranite ; a collison signature of the Himalaya. A model for its genesis and emplacement. J. Geophys. Res. B11, v. 86, p. 10545-10568.
Lusk, J. and Ford, C. E. (1978) Experimental extension of the sphalerite geobarometer to 10 Kbar, Am. Min., v. 63, p. 516-532.
Na, C. K. (1994) unpurblished doctor thesis, Univ. Tsukuba, Japan.
Nakai, S. (1992) Recent developements in dating mineralizations. Geochemistry (Japan), v. 26, p. 51-61.
Nicholls, J. and Crowford, M. L. (1985) FORTRAN programs for calculation of fluid inclusions of fluid properties from microthermometric data on fluid inclusions, Computers Geosci., v. 11, p. 619-645.
Potter, R. W. and Brown, D. L. (1977) The volumetric properties of aqueous sodium chloride solutions from 0 to 500 at pressures up to 2000bars based on a regression of available data in the literature, U.S. Geo. Survey Bull., v. 1421-E, p. 36.
Scott, S. D. (1973) Experimental calibration of the sphalerite geobarometer, Econ. Geol., v. 68, p. 466-474.
Scott, S. D. and Barnes, H. L. (1971) Sphalerite geothermometry and geobarometry, Econ. Geol., v. 66, p. 653-669.
Turpin, L., Cuney, M., Friedrich, M., Bouchez, J.L. and Aubertin, M. (1990) Meta-igneous origin of hercynian peraluminous granites in N. W. French massif central; implications for crustral history reconstructions. Contrib. Mineral. Petrol., v. 104, p. 163-172.
Yoon, C. H. and Shimazaki, H. (1993) Sulfur isotope study of gold-silver deposits in the Republic of Korea, Resource Geology (Japan), v. 43, p. 1-10.

Manuscript received 8 November 1995

전북 번암광산의 지질과 지화학적 연구

정재일 · 나춘기 · 이영엽 · 전서령 · 김선영

요 약 : 번암광산은 소백산 육괴의 남서부에 위치하며, 소백산은 편마암 복합체를 N20~30°E 방향으로 관입하여 나타난다. 주변 화강암들은 변성화강암류의 재용융 혹은 부분용융에 의해 생성된 calc-alkaline계열의 마그마로부터 분화 생성된 산화물로 추정된다. 광상을 배태시킨 광화용액을 화강암체를 형성한 마그마로부터 유래하였다해도 시기적으로 훨씬 후기에 생성되었을 것이다. 공생광물군에 대한 연구결과 광화작용은 크게 3시기로 I기: 기저 유화광물의 생성시기, II기: 후기 유화광물, 엘렉트럼 및 함은 유염 광물의 생성시기, III기: 소량의 함은 광물, 백색석영 및 탄산염광물의 생성시기로 나눌 수 있다. 번암광산의 생성온도, 염농도 및 압력은 광물공생과 화학성분, 유체포유물, 유황동위원소 지질온도계를 이용하여 측정되었으며 다음과 같다. I기: 200~315℃, 3.5~6.5 NaCl eq. wt.%, 0.28~0.61 Kbar, II기: 150~235℃, 4.5~7.4 NaCl eq. wt.%, 0.11~0.15 Kbar로 나타난다. 초기 광화작용동안산소와 유황분압은 각각, $10^{-35.1}$~$10^{-39.7}$ atm., $10^{-11.0}$~$10^{-13.4}$ atm. 으로 나타난다. 이와 같은 연구결과 번암광산은 polymetallic meso-epithermal type의 광상으로 생각된다.